

Special
Collection

Design and Operation of an Operando Synchrotron Diffraction Cell Enabling Fast Cycling of Battery Materials

Olof Gustafsson,^[a] Alexander Schökel,^[b] and William R. Brant^{*[a]}

Operation of a battery typically involves dynamic and non-equilibrium processes, making real time *operando* techniques crucial for understanding their nature. *Operando* X-ray diffraction is an important technique for investigating metastable intermediates and non-equilibrium phase transitions in crystalline electrode materials. Currently employed experimental setups often apply a disruptive approach to cell design, whereby the integrity of standard electrochemical cells is compromised to facilitate collection of high-quality diffraction data. Here, we present a non-disruptive approach to adapting the use of a standard pouch cell that enables fast and long-term cell cycling. Suitability of the setup is demonstrated on the well-studied cathode material $\text{LiNi}_{0.5}\text{Mn}_{1.5}\text{O}_4$. While exhibiting comparable electrochemical behavior to a standard pouch cell up to a current rate of 8 C ($\sim 6.6 \text{ mA cm}^{-2}$), phase transitions could be monitored accurately. Thus, the cell provides a new alternative to investigating non-equilibrium transitions and long-term aging effects in battery materials.

During operation of a battery many dynamic and non-equilibrium processes take place and effect the performance and degradation of the different material components. Monitoring these processes in real time is essential for understanding and improving battery chemistries. Relaxation back to a thermodynamical equilibrium state during extraction of material for *ex situ* evaluation means that information of the real state during operation can be lost. As such, *operando* characterization techniques are commonly employed to study the complex processes occurring in a battery during operation.^[1] Specifically, structural changes in crystalline electrode materials during charge and discharge may involve

formation of metastable intermediates and non-equilibrium phase transitions. For example, in the $\text{Li}_{1+\delta}\text{Mn}_2\text{O}_4$ system solid solution behavior was observed as an additional feature to the previously known two-phase transition only observed *ex situ*.^[2] Thus, *operando* diffraction techniques are important characterization methods for evaluating the structural behavior of battery materials during operation. *Operando* X-ray diffraction has been particularly useful in identifying new phases appearing in battery materials during cycling at high rates. In the case of the cathode material LiFePO_4 , which exhibits a two-phase reaction upon Li insertion and extraction, *operando* X-ray diffraction was utilized to identify a shift towards a non-equilibrium solid solution reaction when cycled at 5 C.^[3] In the Na analogue, NaFePO_4 , a decrease in the compositional range of the region where three phases coexist and a shift from two consecutive biphasic reactions to a single biphasic reaction upon discharge could be identified from *operando* X-ray diffraction when cycled at 1 C.^[4] Also in the case of $\text{LiNi}_{1/3}\text{Mn}_{1/3}\text{Co}_{1/3}\text{O}_2$, *operando* X-ray diffraction helped identify intermediate phases, previously not observed at low rates ($\leq 1 \text{ C}$), when cycling the material at 10 C.^[5] Particularly interesting in these three examples is the influence of the cycling rate on the structural behavior of the material, which opens up questions on the effects of high cycling rates on the structural behavior in other cathode materials. However, conducting *operando* diffraction studies at high current rates creates demands on the experimental setup. Both from an electrochemical perspective, due to effects such as increased polarization, as well as from a diffraction perspective, with shorter collection times being necessary to resolve and track structural changes adequately.

Cell designs for performing standard electrochemical testing of battery systems within research are often inspired by the commonly available coin, pouch or Swagelok-type cells. While these are highly optimized for electrochemical characterization, transfer of the design to an *operando* X-ray diffraction setup usually requires some modification to the cell architecture. This is due to the need for minimizing the amount of material which is not of interest in the beam pathway. Inactive materials such as casing or housing may contribute with significant absorption or scattering. This limits the quality of the diffraction data by hindering the flux of X-rays reaching the studied active material and also the scattered X-rays. Scattering components inside the battery cell other than the active material studied may also contribute negatively towards the acquired diffraction data in terms of peak overlap. It is however of importance to not significantly disrupt the electrochemical performance of the cell when constructing an *operando* cell. Similar electrochem-

[a] O. Gustafsson, Dr. W. R. Brant
Department of Chemistry – Ångström Laboratory
Uppsala University
75121, Uppsala, Sweden
E-mail: william.brant@kemi.uu.se

[b] Dr. A. Schökel
Deutsches Elektronen Synchrotron (DESY)
Hamburg, 22607, Germany

Supporting information for this article is available on the WWW under <https://doi.org/10.1002/batt.202100126>

An invited contribution to a joint Special Collection between Batteries & Supercaps and Chemistry-Methods on In Situ and Operando Methods for Energy Storage and Conversion

© 2021 The Authors. Batteries & Supercaps published by Wiley-VCH GmbH. This is an open access article under the terms of the Creative Commons Attribution Non-Commercial License, which permits use, distribution and reproduction in any medium, provided the original work is properly cited and is not used for commercial purposes.

ical performance to optimized cells ultimately enables accurate structure-property relationships to be determined.

A popular *operando* cell design are modified coin cells. A common modification consists of drilling a hole in the coin cell casing and sealing with Kapton® tape. This solution was employed in the previously mentioned study of $\text{LiNi}_{1/3}\text{Mn}_{1/3}\text{Co}_{1/3}\text{O}_2$.^[5] Problems with this approach are associated with a loss of stack pressure due to the flexibility of the tape material, along with oxidation of the Kapton® and an increase in the cell resistance, limiting the electrochemical performance.^[6] Permeability of air and moisture through the Kapton® tape also acts as a limitation towards shorter studies using this design approach.^[1a] A modified approach to this design was employed, using metal tapes instead of Kapton®, with results showing an improved electrochemical performance, comparable to an unmodified coin cell.^[6a] Another modification to the coin cell design is thinning of the casing using laser-etching.^[7] While providing good electrochemical performance, comparable to that of a standard coin cell, the technique required for modification of the cell might not be readily available to most users and institutions. One design to overcome issues of low stack pressure while remaining hermetically sealed is the so called AMPIX cell, developed at the Argonne National Laboratory for use at the Advanced Photon Source.^[8] The cell design simultaneously provides a low background to the diffracted pattern and a uniform stack pressure due to the use of glassy carbon windows. The cell is compatible with multiple scattering techniques, not only limited to X-ray diffraction. The AMPIX cell was utilized in the previously mentioned study on LiFePO_4 , where the active material was cycled in the form of a pellet.^[3] The use of a pelletized electrode and the many different interfaces in the AMPIX cell could be a drawback for high-rate studies however, due to sluggish mass transport in pellet electrodes and increased resistance from multiple interfaces.^[9] As of now, there is a gap to be filled in the currently available designs, providing a unified solution to conducting both long term and high rate *operando* X-ray diffraction studies in a facile way. Specifically, the need for accessible setups where the advanced equipment and high energy X-rays needed for utilizing the laser-etched coin cell design are not available. Employing a pouch cell for these types of studies could aid in filling this gap. As for pouch cell setups, the main issue lies within the need for applying external stack pressure, often in the form of plates and clamps on either side of the cell. While the pouch cell has a lower amount of inactive material compared to a coin cell and Swagelok-type cell, the need for external stack pressure complicates its use within *operando* X-ray diffraction setups, since a low stack pressure can limit the maximum current density feasible. Introduction of external stack pressure can also lead to more inactive material in the beam pathway which needs to be tailored as to reduce unwanted scattering and absorption. However, if the issue with applied stack pressure can be solved for a pouch cell setup, the highly optimized design towards electrochemical performance can be utilized for *operando* X-ray diffraction studies at high current rates and long-term studies. Adaptations aimed at solving this issue for pouch cell setups have been done by

modifying the cell, including a Ti or Al plate inside the pouch in combination with an outer wave spring to provide stack pressure.^[10] While solving the issue of stack pressure for a pouch cell setup, the approach taken is disruptive toward the pouch cell design and construction may not be trivial. Another approach was recently taken, where stack pressure was applied by sandwiching a standard pouch cell between two 250 μm thick Be plates, which were then pressurized externally.^[11] How the stack pressure was set and controlled in this design remains unclear however.

In this study we present a non-disruptive approach towards optimizing the pouch cell type design for battery *operando* X-ray diffraction measurements. The approach takes advantage of the high energy and flux available at synchrotron facilities, showing that the commonly used pouch cell design can be utilized in an unmodified way to simultaneously achieve good quality diffraction data and representative electrochemical performance. The presented cell design allows for a set stack pressure, which can be tuned by the user. The cell design was utilized on the P02.1 beamline at the PETRA III synchrotron facility (DESY, Hamburg), studying the structural behavior of $\text{LiNi}_{0.5}\text{Mn}_{1.5}\text{O}_4$ during galvanostatic cycling at current rates of 1 C and 8 C. The commonly known phase transitions could be tracked during cycling and cell parameters and weight fractions of the different $\text{Li}_x\text{Ni}_{0.5}\text{Mn}_{1.5}\text{O}_4$ phases could be extracted. Furthermore, the suitability of the cell design for other *operando* techniques such as Bragg coherent diffractive imaging and X-ray absorption spectroscopy as well as spatially resolved studies are considered.

In the presented setup, a standard pouch cell is assembled in a holder which provides a controllable and reproducible stack pressure by means of a wave spring and glassy carbon windows, see Figure 1. Since the compression length of the wave spring is fixed in the setup, the applied stack pressure can be optimized by changing the wave spring constant (k), see Table 1. Alternatively, the stack pressure can be modified by the compression length of the wave spring, controlled by the interchangeable spacers in the setup. See Supporting Information for details on the calculation of applied stack pressure.

It should be noted that the calculated stack pressure is the theoretically applied stack pressure. Due to the compressibility of the cell components, the real applied stack pressure can reasonably be assumed to be smaller.^[12] Measuring the real applied stack pressure is not trivial and typically requires a more extensive setup including a load cell or force sensor, which was not further explored here.^[12–13] Homogeneity in the stack pressure can be reasonably assumed due to the rigidity of

Table 1. Resulting theoretically applied stack pressure in the *operando* pouch cell holder as a function of the wave spring constant, k , for various values of k .

Wave spring constant, k [N/mm]	Applied stack pressure [MPa]
5	0.11
25	0.53
50	1.05

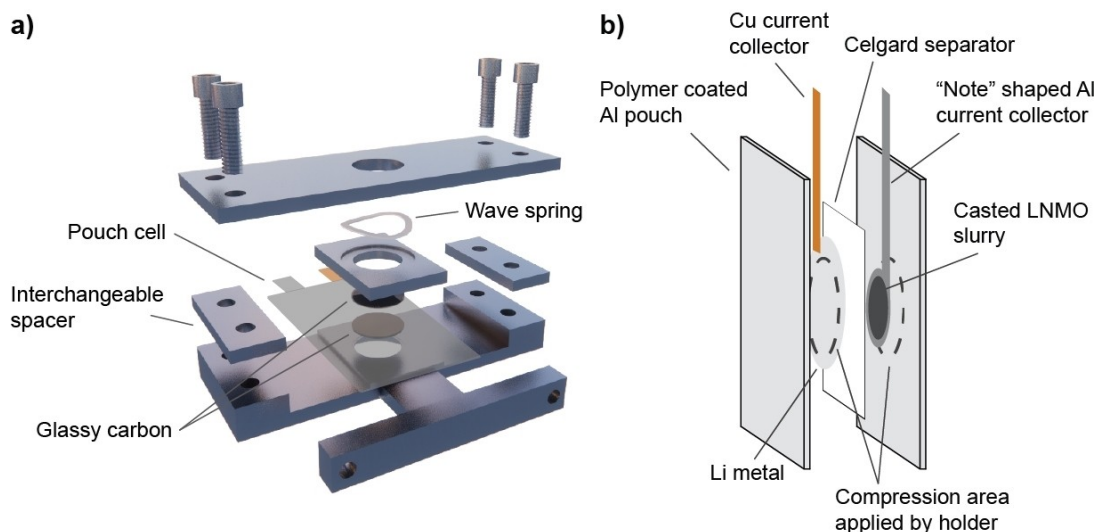


Figure 1. Design and principle sketch of a) the *operando* pouch cell holder setup and b) schematic design of the pouch cell.

the glassy carbon windows and the flat compressed area. Further, given the high energy of the X-rays (~ 60 keV) utilized in this study, inhomogeneity in the reaction state across the electrode is not expected.^[6b] Confirming homogeneity in the reaction state across the electrode in a similar manner as was done by Borkiewicz et al. would be interesting, but remain outside the scope of this study.^[6b] The pouch cell cycled in the *operando* cell holder was benchmarked against a pouch cell cycled in-house, utilizing a standardized setup with stack pressure applied from plates and clamps. The resulting voltage profiles of galvanostatic charge and discharge at current rates 1 C and 8 C are shown in Figure 2, indicating similar achieved voltage profiles and capacities. The glassy carbon windows provide mechanical rigidity for the setup while only contributing with an easily modeled background in the collected diffraction pattern, see Figure S1. The choice of window material here was done due to the low cost and ease of handling the material. Other window materials, for example Be, diamond or sapphire, could be employed based on the needs for the specific material or cell chemistry studied. Especially since the window material is not in contact with the cell chemistry, issues with side reactions, for example oxidation from the electrolyte, are avoided. This highlights the versatility of the presented design. By moving the Cu current collector out of the beam pathway inside the pouch cell, its contribution to the diffracted pattern is removed, leaving only Al from the pouch material and the positive electrode material current collector as a contributor to the diffracted pattern (Figure 3a). This might not be possible in some cases when studying for example full cells, where the Cu current collector will sit in the beam pathway, unless a self-supporting and conducting electrode is employed. In these cases, it is important to take into consideration and account for possible peak overlap and reduced X-ray transmission due to the absorption from Cu.

Synchrotron *operando* X-ray diffraction measurements on $\text{LiNi}_{0.5}\text{Mn}_{1.5}\text{O}_4$ (LNMO) half cells with Li foil as negative electrode were performed on the P02.1 beam line at Petra III (DESY,

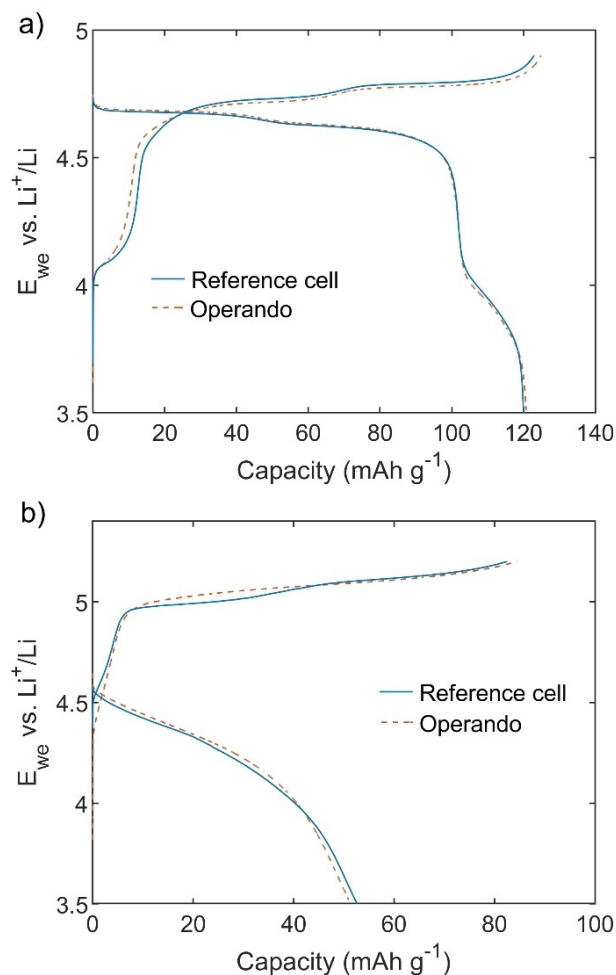


Figure 2. Voltage profiles during galvanostatic cycling at rates a) 1 C and b) 8 C of a reference pouch cell cycled in-house and a cell cycled in the pouch cell holder.

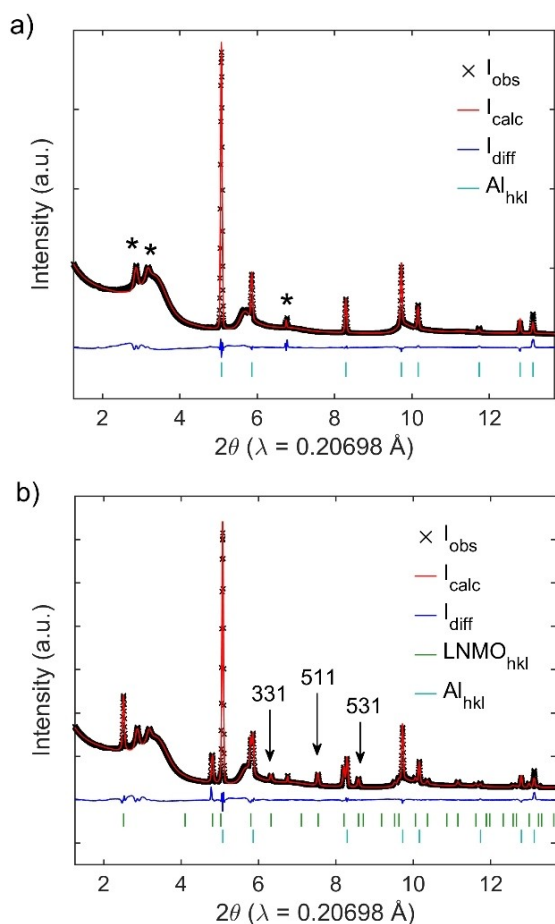


Figure 3. a) Observed and calculated X-ray diffraction pattern from Rietveld refinement of a pouch cell in the holder, without active material, i.e. $\text{LiNi}_{0.5}\text{Mn}_{1.5}\text{O}_4$. Peaks indicated with * are associated with the polymer separator. b) Observed and calculated X-ray diffraction pattern from Rietveld refinement of a pouch cell in the holder with active material, i.e. $\text{LiNi}_{0.5}\text{Mn}_{1.5}\text{O}_4$. The 311, 511 and 531 reflections are indicated with arrows.

Hamburg) at different galvanostatic cycling rates. A resulting diffracted and calculated pattern from Rietveld refinement of LNMO in a pouch cell assembled in the cell holder is shown in Figure 3b. The contribution from the glassy carbon windows, Al and polymer separator can be accounted for in the calculated pattern, while simultaneously modeling the contribution from LNMO. Contribution towards the diffracted pattern from the electrolyte was limited to the background and could be readily included in the modeled background.

The contribution from the glassy carbon windows was modeled as a custom background using the macro *bkg_file* in TOPAS V6,^[14] see Supporting Information for an example of the .inp-file used in refinements. Furthermore, structural changes during galvanostatic charge and discharge could be monitored *operando* in LNMO at cycling rates 1 C ($\sim 0.8 \text{ mA cm}^{-2}$) and 8 C ($\sim 6.6 \text{ mA cm}^{-2}$) respectively, exemplified by the evolution of the 331, 511 and 531 reflections, as shown in Figure 4. Cell parameter (*a*) and weight fractions of the individual $\text{Li}_x\text{Ni}_{0.5}\text{Mn}_{1.5}\text{O}_4$ phases (Phase I, Li rich, and Phase II, Li poor) during cycling at 1 C were extracted using sequential refinements in TOPAS V6, see Figure 5. The previously known solid

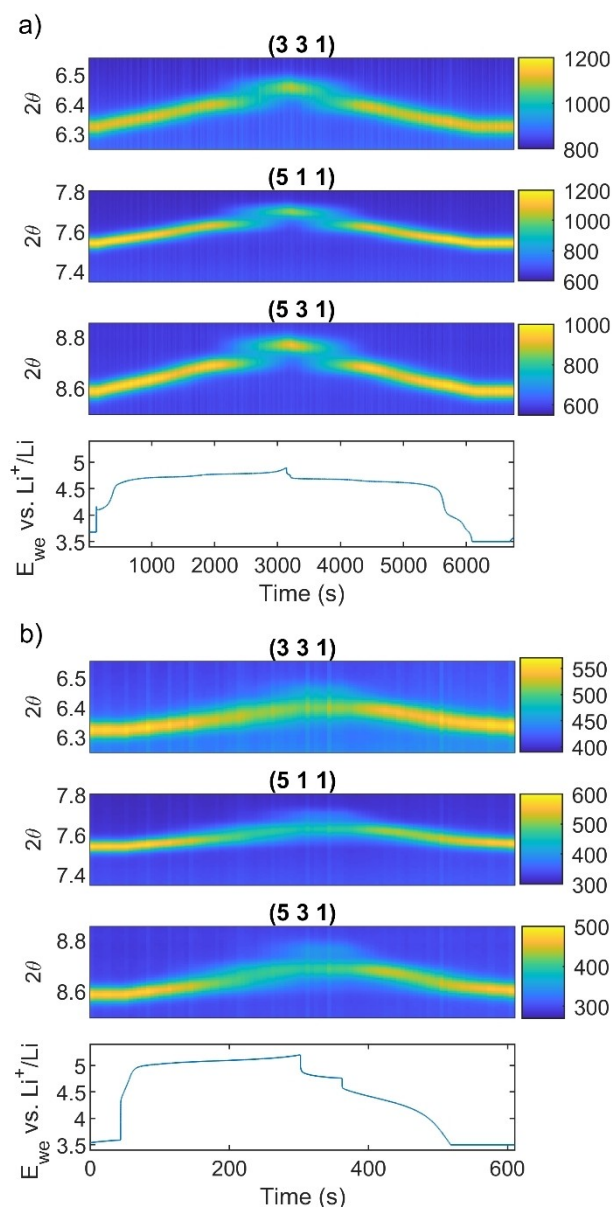


Figure 4. Diffraction heatmap and galvanostatic cycling curve of $\text{LiNi}_{0.5}\text{Mn}_{1.5}\text{O}_4$ at a cycling rate of a) 1 C and b) 8 C, tracking changes in the 331, 511 and 531 reflections. The collection time for each pattern was 10 seconds and 5 seconds at 1 C and 8 C, respectively.

solution and two-phase reaction of LNMO upon Li extraction and insertion could be confirmed in both cases and thus showcases the suitability of the experimental setup for these types of studies.^[15] Even at a relatively high C-rate of 8 C, structural changes could be monitored with a collection time of five seconds per pattern. While even higher rates are possible to study for LNMO, they are typically limited to discharge due to the high polarization occurring on charge at high current rates.^[16] It should be noted however, based on the comparable electrochemical performance to a standard pouch cell, reaching higher cycling rates than those reported in the present study becomes dependent on the material studied, its morphology and the chosen cell chemistry, for example choice

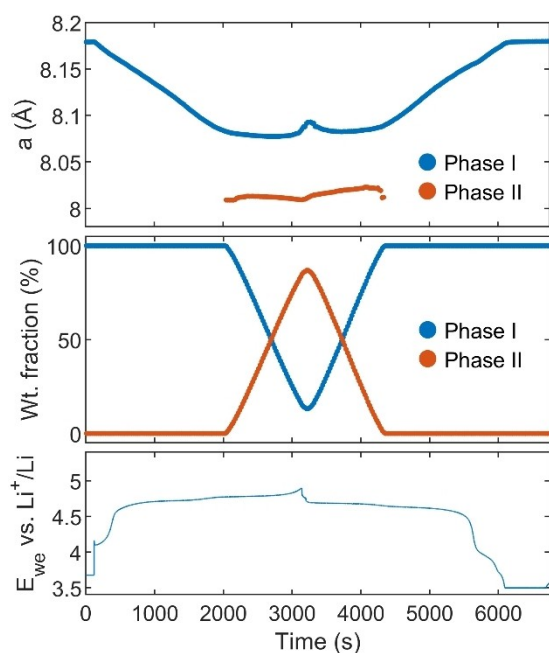


Figure 5. Evolution of the refined cell parameter, a , and weight fraction of Li rich (Phase I) and Li poor (Phase II) phases in $\text{Li}_x\text{Ni}_{0.5}\text{Mn}_{1.5}\text{O}_4$ during galvanostatic cycling at a rate of 1 C.

of cathode, anode, electrolyte and salt etc., and is less influenced by the *operando* cell design presented here. This highlights the setups suitability for performing studies of battery materials at high rates.

It is worth noting that, due to the ongoing pandemic situation, these synchrotron *operando* measurements were performed remotely with the help of beamline staff. All pouch cells were prepared and pre-cycled in-house before being shipped to and assembled in the pouch cell holder on site at PETRA III without prior training on the setup. This highlights the simplicity of the cell setup and the ability to perform collaborative high-quality studies at a distance. Furthermore, the lack of need for pouch cell assembly on site opens up the possibility of studying pre-aged cells which have been extensively cycled in-house prior to the allocated beamtime.

Considering the use of the demonstrated cell design for other types of X-ray studies the absorption was calculated exemplarily for use in studying the extended X-ray absorption fine structure (EXAFS) at the Ni K-edge. Based on an active material (LNMO) loading of $\sim 8 \text{ mg/cm}^2$ the resulting transmission would amount to $\sim 8\%$ with an edge step of ~ 0.4 , thus making the cell design suitable for these types of measurements. See Supporting Information for more information regarding the calculations on the X-ray absorption. To increase transmittance further, Al free pouch cell material could be considered for short term X-ray absorption studies (Figure S2). Other window materials, such as Be, can also be utilized based on the specific needs for the type of measurement carried out.

Further, the cell design demonstrates potential for use with techniques such as Bragg coherent diffractive imaging (BCDI). Previous investigations utilized a modified coin cell with Kapton® tape windows to study topological defects in LNMO.^[17]

Since replacing a modified coin cell with our pouch cell design does not significantly reduce the diffracted signal for *operando* diffraction experiments, our cell would be suitable for BCDI experiments as well. In particular, by eliminating the use of a window it opens for opportunities to study material behavior at higher rates or during long-term operation. Also, access to the whole 13 mm diameter electrode in the presented design opens up opportunities for conducting spatially resolved diffraction, total scattering, spectroscopic or BCDI studies of whole electrodes.

To summarize, we present an experimental setup for *operando* X-ray diffraction studies, utilizing the robust electrochemical performance of a pouch cell in combination with a low background cell holder with controlled stack pressure. The non-disruptive nature of the cell design enables high rate studies while maintaining electrochemical performance comparable to that of a standard pouch cell. The cell design provides reproducible and easily modeled contributions to the diffracted pattern which allows for good quality X-ray diffraction data. This will be helpful for studying non-equilibrium and metastable states in battery materials, especially at high rates, aiding the understanding of the underlying mechanisms and their link to battery performance.

Acknowledgements

Leif Edlén is acknowledged for technical assistance in the construction of the *operando* pouch cell holder. Haldor Topsoe is acknowledged for providing material for this study. The authors would also like to thank James Brant for preparing the 3D renders in Figure 1 and table of content image. The authors also gratefully acknowledge funding from the Strategic Research Area StandUp for Energy and the Swedish Energy Agency (grant no. 48678-1). We acknowledge DESY (Hamburg, Germany), a member of the Helmholtz Association HGF, for the provision of experimental facilities. Parts of this research were carried out at PETRA III using beamline P02.1.

Conflict of Interest

The authors declare no conflict of interest.

Keywords: *operando* • X-ray diffraction • spinel phases • structural analysis • fast cycling

- [1] a) D. Liu, Z. Shadike, R. Lin, K. Qian, H. Li, K. Li, S. Wang, Q. Yu, M. Liu, S. Ganapathy, X. Qin, Q.-H. Yang, M. Wagemaker, F. Kang, X.-Q. Yang, B. Li, *Adv. Mater.* **2019**, *31*, 1806620; b) S.-M. Bak, Z. Shadike, R. Lin, X. Yu, X.-Q. Yang, *NPG Asia Mater.* **2018**, *10*, 563–580; c) M. Wolf, B. M. May, J. Cabana, *Chem. Mater.* **2017**, *29*, 3347–3362; d) W. Li, D. M. Lutz, L. Wang, K. J. Takeuchi, A. C. Marschillok, E. S. Takeuchi, *Joule* **2021**, *5*, 77–88; e) F. Lin, Y. Liu, X. Yu, L. Cheng, A. Singer, O. G. Shpyrko, H. L. Xin, N. Tamura, C. Tian, T.-C. Weng, X.-Q. Yang, Y. S. Meng, D. Nordlund, W. Yang, M. M. Doeff, *Chem. Rev.* **2017**, *117*, 13123–13186; f) Z. Shadike, E. Zhao, Y.-N. Zhou, X. Yu, Y. Yang, E. Hu, S. Bak, L. Gu, X.-Q. Yang, *Adv. Energy Mater.* **2018**, *8*, 1702588; g) A. M. Tripathi, W.-N. Su, B. J. Hwang,

- Chem. Soc. Rev.* **2018**, *47*, 736–851; h) E. Hu, X. Wang, X. Yu, X.-Q. Yang, *Acc. Chem. Res.* **2018**, *51*, 290–298; i) P. Ghigna, E. Quartarone, *J. Phys. Energy* **2021**, *3*, 032006.
- [2] B. Song, G. M. Veith, J. Park, M. Yoon, P. S. Whitfield, M. J. Kirkham, J. Liu, A. Huq, *Chem. Mater.* **2019**, *31*, 124–134.
- [3] H. Liu, F. C. Strobridge, O. J. Borkiewicz, K. M. Wiaderek, K. W. Chapman, P. J. Chupas, C. P. Grey, *Science* **2014**, *344*.
- [4] D. Saurel, M. Galceran, M. Reynaud, H. Anne, M. Casas-Cabanas, *Int. J. Energy Res.* **2018**, *42*, 3258–3265.
- [5] Y.-N. Zhou, J.-L. Yue, E. Hu, H. Li, L. Gu, K.-W. Nam, S.-M. Bak, X. Yu, J. Liu, J. Bai, E. Dooryhee, Z.-W. Fu, X.-Q. Yang, *Adv. Energy Mater.* **2016**, *6*, 1600597.
- [6] a) G. Liang, J. Hao, A. M. D'Angelo, V. K. Peterson, Z. Guo, W. K. Pang, *Batteries & Supercaps* **2021**, *4*, 380–384; *Supercaps* **2021**, *4*, 380–384; b) O. J. Borkiewicz, K. M. Wiaderek, P. J. Chupas, K. W. Chapman, *J. Phys. Chem. Lett.* **2015**, *6*, 2081–2085.
- [7] C. Xu, K. Märker, J. Lee, A. Mahadevegowda, P. J. Reeves, S. J. Day, M. F. Groh, S. P. Emge, C. Ducati, B. Layla Mehdi, C. C. Tang, C. P. Grey, *Nat. Mater.* **2021**, *20*, 84–92.
- [8] O. J. Borkiewicz, B. Shyam, K. M. Wiaderek, C. Kurtz, P. J. Chupas, K. W. Chapman, *J. Appl. Crystallogr.* **2012**, *45*, 1261–1269.
- [9] M. Gaberscek, J. Moskon, B. Erjavec, R. Dominko, J. Jamnik, *Electrochem. Solid-State Lett.* **2008**, *11*, A170.
- [10] C. Villevieille, T. Sasaki, P. Novák, *RSC Adv.* **2014**, *4*, 6782–6789.
- [11] J. Park, H. Zhao, S. D. Kang, K. Lim, C.-C. Chen, Y.-S. Yu, R. D. Braatz, D. A. Shapiro, J. Hong, M. F. Toney, M. Z. Bazant, W. C. Chueh, *Nat. Mater.* **2021**, *20*, 991–999.
- [12] V. Müller, R.-G. Scurtu, M. Memm, M. A. Danzer, M. Wohlfahrt-Mehrens, *J. Power Sources* **2019**, *440*, 227148.
- [13] J. Cannarella, C. B. Arnold, *J. Power Sources* **2014**, *245*, 745–751.
- [14] A. Coelho, *J. Appl. Crystallogr.* **2018**, *51*, 210–218.
- [15] J. H. Kim, S. T. Myung, C. S. Yoon, S. G. Kang, Y. K. Sun, *Chem. Mater.* **2004**, *16*, 906–914.
- [16] X. Hao, B. M. Bartlett, *J. Electrochem. Soc.* **2013**, *160*, A3162–A3170.
- [17] A. Ulvestad, A. Singer, J. N. Clark, H. M. Cho, J. W. Kim, R. Harder, J. Maser, Y. S. Meng, O. G. Shpyrko, *Science* **2015**, *348*, 1344.

Manuscript received: June 4, 2021

Revised manuscript received: July 9, 2021

Accepted manuscript online: July 12, 2021

Version of record online: July 23, 2021